Transition-Metal Complexes

Deutsche Ausgabe: DOI: 10.1002/ange.201500792
Internationale Ausgabe: DOI: 10.1002/anie.201500792

True Boundary for the Formation of Homoleptic Transition-Metal Hydride Complexes**

*Shigeyuki Takagi, Yuki Iijima, Toyoto Sato, Hiroyuki Saitoh, Kazutaka Ikeda, Toshiya Otomo, Kazutoshi Miwa, Tamio Ikeshoji, Katsutoshi Aoki, and Shin-ichi Orimo**

Abstract: *Despite many exploratory studies over the past several decades, the presently known transition metals that form homoleptic transition-metal hydride complexes are limited to the Groups 7–12. Here we present evidence for the formation of Mg_3CrH_8, containing the first Group 6 hydride complex $[CrH_7]^{5-}$. Our theoretical calculations reveal that pentagonal-bipyramidal H coordination allows the formation of σ-bonds between H and Cr. The results are strongly supported by neutron diffraction and IR spectroscopic measurements. Given that the Group 3–5 elements favor ionic/metallic bonding with H, along with the current results, the true boundary for the formation of homoleptic transition-metal hydride complexes should be between Group 5 and 6. As the H coordination number generally tends to increase with decreasing atomic number of transition metals, the revised boundary suggests high potential for further discovery of hydrogen-rich materials that are of both technological and fundamental interest.*

Hydrogen, despite being the simplest element, has a rich chemistry which allows it to form various chemical bonds in materials. The flexibility of hydrogen results in a varied set of functionalities, including hydrogen storage,[1] superconductivity,[2] fast ionic conductivity,[3] magnetism,[4] and metal–insulator transitions.[5] Besides the technological importance, there is current interest in unraveling the interplay between compositions, structure, and chemical bonding associated with hydrogen that often provokes controversy.[6] This is particularly stimulated by recent findings regarding hydrogen incorporated in oxide hosts, which revealed the true oxidation state of hydride ions hidden by hydroxide ions.[7]

The flexibility of hydrogen appears prominently in hydrogen–metal interactions. In particular, hydrogen as a ligand (hydride ligand) is extremely versatile,[8] forming a varied set of homoleptic transition-metal hydride complexes that display a remarkably rich variety of H coordination modes, ranging from twofold to ninefold.[9] These complexes are stabilized by charge transfer from electropositive counterions to form insulating hydrides (complex transition-metal hydrides).[10,11a] The versatility of the hydride ligand is derived mainly from the specific electronegativity of H, which is much closer to those of transition metals, as compared with typical electronegative elements, such as nitrogen, oxygen, and fluorine.[12] This then allows for substantial hybridization between the H 1s and transition-metal spd orbitals to form strong σ-bonds with the aid of ligand field effects.

At the same time, despite a number of exploratory studies over the past several decades, the presently known elements that form such complexes are limited to transition metals ranging from Group 7–12.[9] One possible explanation of this limitation is that the electronegativity in the periodic table tends to decrease when going from right to left along a period; thus, the relatively electropositive early transition metals favor ionic/metallic bonding with hydrogen, instead of covalent bonding as in hydride complexes. In fact, Group 3–5 elements form stable binary metal hydrides, in which hydrogen interstitially incorporates into the metal lattice (interstitial H), which would be an undesired competing reaction to the formation of hydride complexes. Furthermore, it was reported that these elements also form ternary metal hydrides with magnesium instead of transition-metal hydride complexes, even under high temperature and pressure (on the order of several GPa).[13] These experimental data imply the difficulty in formation of early transition-metal hydride complexes; however, the possibility for the formation of Group 6 hydride complexes cannot be ruled out.

Generally the H coordination number tends to increase with decreasing valence electron count of transition metals to accommodate the 18-electron rule. Indeed, the highest H coordination number known is found only in Group 7 hydride

[*] Dr. S. Takagi, Y. Iijima, Dr. T. Sato, Dr. K. Aoki, Prof. Dr. S. Orimo
Institute for Materials Research, Tohoku University
Sendai 980-8577 (Japan)
E-mail: orimo@imr.tohoku.ac.jp
Dr. H. Saitoh
Quantum Beam Science Directorate (Japan) Atomic Energy Agency
Hyogo 679-5148 (Japan)
Dr. K. Ikeda, Prof. Dr. T. Otomo
Institute of Materials Science
High Energy Accelerator Research Organization
Tsukuba 305-0801 (Japan)
Dr. K. Miwa
Toyota Central R&D Laboratories, Inc.
Nagakute 480-1192 (Japan)
Dr. T. Ikeshoji, Prof. Dr. S. Orimo
WPI-Advanced Institute for Materials Research, Tohoku University
Sendai 980-8577 (Japan)

[**] We are grateful for helpful discussions with D. Noréus, technical support from R. Hiraoka and H. Ohmiya, and the use of SR16000 supercomputing resources at the Center for Computational Materials Science of the Institute for Materials Research, Tohoku University. The neutron scattering experiment was approved by the Neutron Scattering Program Advisory Committee of IMSS, KEK (Proposal No. 2014S06). This work was supported by JSPS KAKENHI (grant numbers 26820312, 25220911, and 26820313) and the Photon and Quantum Basic Research Coordinated Development Program by MEXT.

Supporting information for this article is available on the WWW under http://dx.doi.org/10.1002/anie.201500792.

complexes, $[TcH_9]^{2-}$ and $[ReH_9]^{2-}$.[9] Thus, if the Group 6 elements prove to form the hydride complexes, the higher H coordination number than ever can be expected. Such the hydrogen-rich materials would be of interest from a point of view of high-T_c superconductivity, because the H 1s derived states, which dominate the valence bands, have already undergone a form of chemical precompression,[2a] leading to the metallization at a pressure much lower than that predicted for pure hydrogen;[2b] for example, $BaReH_9$, containing $[ReH_9]^{2-}$, was theoretically predicted to turn metallic with evolution of discrete H_2 units in the structure above 51 GPa.[14]

In this communication, we theoretically examine the possibility for the formation of homoleptic hydride complexes of the Group 6 element chromium, using first-principles density-functional theory (DFT) calculations, followed by experimental examination. Mg was chosen as a counterion because it stabilizes the hydride complexes of 3d transition metals from Group 7–10, forming complex transition-metal hydrides: Mg_3MnH_7 ($Mg^{2+}{}_3[MnH_6]^{5-}H^-$), Mg_2FeH_6 ($Mg^{2+}{}_2[FeH_6]^{4-}$), Mg_2CoH_5 ($Mg^{2+}{}_2[CoH_5]^{4-}$), and Mg_2NiH_4 ($Mg^{2+}{}_2[NiH_4]^{4-}$).[9] These hydrides show an increasing trend in H stoichiometry with decreasing atomic number of transition metals. From this, we speculate that eight H atoms will stabilize our current material. Furthermore, given that a sevenfold H coordination[11] and incorporated H^- ions[1c,10g] stabilize the transition-metal hydride complexes, the composition of the current material can be expected as Mg_3CrH_8 ($Mg^{2+}{}_3[CrH_7]^{5-}H^-$).

We first performed structure determination of hypothetical Mg_3CrH_8 using first-principles calculations (see Section 1 in the Supporting Information (SI) for details of the procedures); Figure 1a illustrates the calculated crystal structure. The material has a pentagonal-bipyramidal CrH_7 unit, with D_{5h} point group symmetry (Figure 1b), and an isolated H atom, occurring in an orthorhombic structure. The average Cr–H length in the CrH_7 unit is 1.67 Å, which is comparable to those in other transition-metal hydride complexes.[9] The H–H nearest neighbor distance on the pentagonal plane of the CrH_7 unit is 1.96 Å. This is much shorter than those in most metal hydrides, which generally have a H–H distance longer than 2.1 Å (Westlake criterion[15]), indicating a different type of chemical bonding from interstitial H. These results support that the bonding in the CrH_7 unit is similar to those in other transition-metal hydride complexes. The calculated crystallographic parameters are summarized in Table S1.

To obtain a better understanding of the cohesion, we examined the electronic structure. Figure 2a shows the calculated electronic density of states (DOS). We checked for the magnetic state, but found no magnetic ordering.

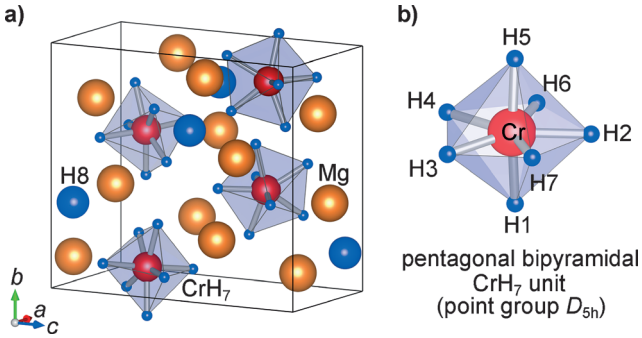

Figure 1. Calculated crystal structure of hypothetical Mg_3CrH_8. a) Mg_3CrH_8 occurs in an orthorhombic structure with space group $P2_12_12_1$ (No. 19). Mg atoms are shown by large orange spheres, Cr by medium red spheres, H coordinating Cr by smaller blue spheres and isolated H by large blue spheres. b) Pentagonal-bipyramidal CrH_7 unit with sevenfold H coordination of Cr.

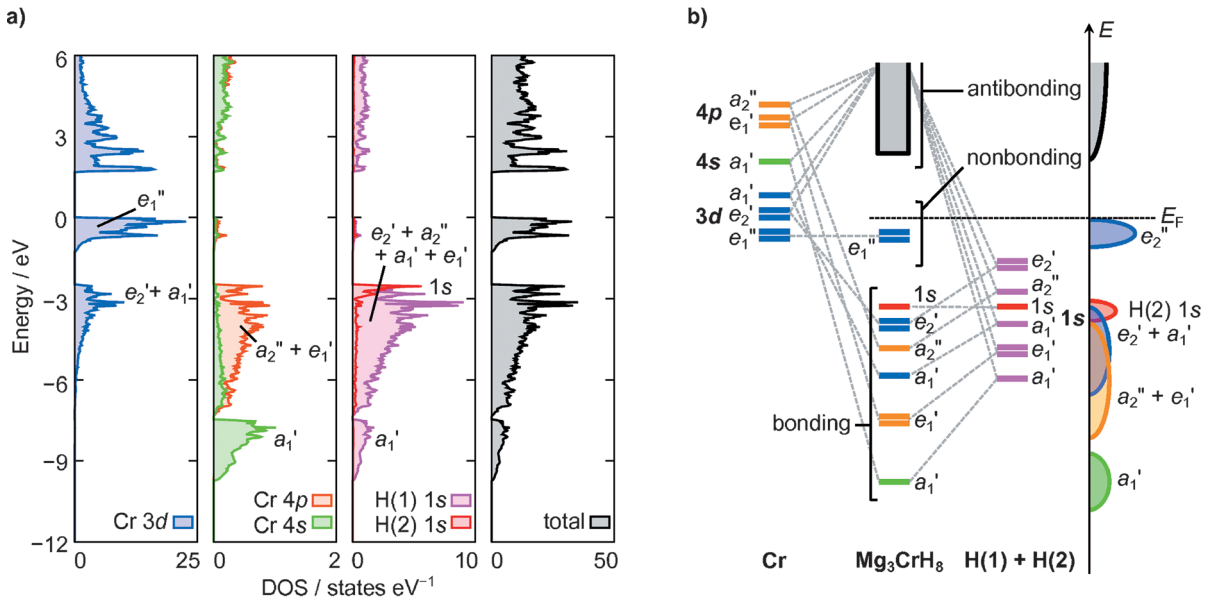

Figure 2. Calculated electronic structure of hypothetical Mg_3CrH_8. a) Electronic DOS. The Cr 3d, Cr 4p, Cr 4s, H(1) 1s, and H(2) 1s projections along with total DOS. b) Schematic depiction of the formation of electronic structure. Zero energy is set at the valence-band maximum.

As can be seen in the rightmost panel of Figure 2a, the valence bands are divided into three parts. These are the lowest-lying DOS from −9.8 to −7.3 eV, the medium-lying DOS from −7.2 to −2.4 eV, and the highest-lying DOS from −1.5 eV to the valence band edge. These are separated from the conduction bands by a gap of 1.7 eV. The lowest-lying DOS is derived from mixing of the 1s orbital of seven H atoms coordinating Cr (H1–H7 in Figure 1, hereafter referred to as H(1)) and Cr 4s orbitals, as can be seen from the H(1) 1s and Cr 4s characters in the corresponding DOS. There is also a strong mixing of the H(1) 1s, Cr 3d, and Cr 4p orbitals in the medium-lying DOS. Meanwhile, the 1s orbitals of isolated H (H8 in Figure 1, hereafter referred to as H(2)) do not hybridize with the Cr orbitals, as is evident from the absence of any band splitting, giving rise to the DOS peak centered at −2.6 eV. Similarly, the highest-lying DOS consists of mostly Cr 3d character without noticeable contributions from H 1s orbitals.

The above-mentioned features of the electronic structure can be understood on the basis of ligand field effects, as schematically illustrated in Figure 2b. In the pentagonal-bipyramidal ligand field, the Cr orbitals are split into a total of six states consisting of: a_2'' and e_1' symmetry states derived from the Cr 4p orbitals, a_1' symmetry state resulting from the Cr 4s orbital, and a_1', e_2', and e_1'' symmetry states split away from the Cr 3d orbitals. Meanwhile, the seven H(1) 1s orbitals form a linear combination of $e_2'+a_2''+a_1'+e_1'+a_1'$. The states possessing the same symmetry hybridize to form five manifolds of bonding states comprised of e_2', a_2'', a_1', e_1', and a_1', and the corresponding antibonding states. The Cr 3d derived e_1'' states and H(2) 1s orbitals remain nonbonding because of the absence of orbitals of the same symmetry, and occur between the bonding and antibonding states. As the current material contains 20 electrons, all the bonding and nonbonding states are fully occupied and the Fermi level falls in the gap between the nonbonding e_1'' and antibonding states. The absence of occupation of any antibonding states suggests that a covalent bond is formed between Cr and H(1), whereas H(2) exists as H^- ion because the nonbonding H(2) 1s derived state is filled with two electrons, giving it an additional electron. The electropositive Mg orbitals occur further above the antibonding states and are not shown here. Thus, the basic building blocks of Mg_3CrH_8 are a covalently bonded $[CrH_7]^{5-}$ unit and an isolated H^- ion, stabilized by charge transfer from Mg to form an ionic configuration of $Mg^{2+}{}_3[CrH_7]^{5-}H^-$, as expected. This is reminiscent of the ionic configuration of Mg_3MnH_7, which also has a 20-electron count with an isolated H^- ion.[10g]

We then demonstrated the formation of the homoleptic hydride complex of Cr experimentally. A mixture of Cr powder and MgH_2 (MgD_2) was hydrogenated (deuterated) under 5 GPa at 973 K for 4 h. The obtained sample had a dark red color, implying the insulating character. The deuteride recovered at ambient pressure and temperature was characterized by powder neutron diffraction (PND), and the obtained profile is depicted in Figure 3b along with the profile simulated using the DFT structure of deuterium-substituted hydride (Figure 3a). As can be seen in Figure 3, the two profiles are practically identical, indicating the successful synthesis of the theoretically predicted Mg_3CrH_8. We performed Rietveld refinement on the profile and obtained a structure very similar to the one obtained from DFT calculations.[16] The procedures for syntheses and PND measurement are shown in Section 1, and the refined crystallographic parameters are summarized in Table S2 in the SI.

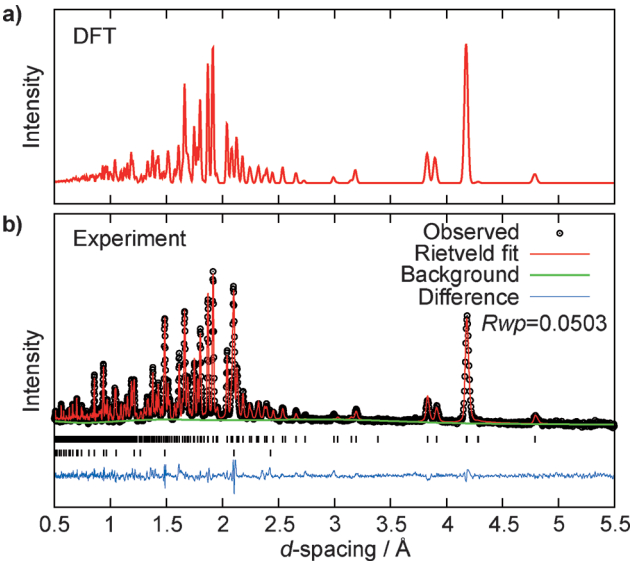

Figure 3. PND profiles of Mg_3CrD_8. a) Simulated profile from hypothetical DFT structure of deuterium-substituted hydride. b) Experimental profile. The positions of Bragg reflection (tick marks) are shown for Mg_3CrD_8 (upper, 79.99(14) wt%) and MgO (lower, 20.01(14) wt%).

Figure 4a and b shows the theoretical and experimental IR spectra of Mg_3CrH_8, respectively, along with the experimentally measured spectrum of Mg_3CrD_8 depicted in Fig-

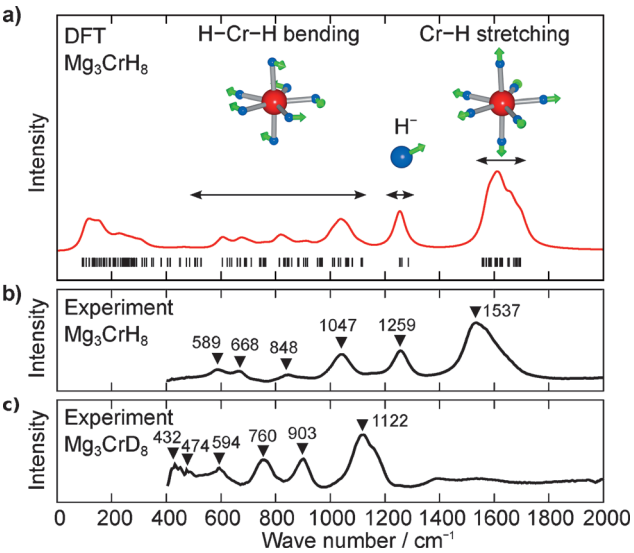

Figure 4. Theoretical and experimental IR spectra. a) IR spectrum of Mg_3CrH_8 obtained from DFT calculations. All the zone-center optic phonon frequencies (144 modes), including those of IR-inactive modes, are shown by tick marks as a reference. b) Experimental IR spectrum of Mg_3CrH_8. c) Experimental IR spectrum of Mg_3CrD_8.

ure 4c (see Section 1 in the SI for details of the procedures). As the primitive cell consists of 48 atoms, there is a total of 141 zone-center optic phonon modes ($36A + 35B_1 + 35B_2 + 35B_3$), as shown by tick marks in Figure 4a. Among them, the modes with frequencies ranging from 1550 to 1700 cm^{-1} originate from the Cr–H stretching vibrations, whereas those in the frequency range between 500 and 1110 cm^{-1} are related primarily to the H–Cr–H bending vibrations. It is worth noting that the modes associated with the isolated H motions are well separated from the Cr–H stretching and H–Cr–H bending vibrations, and falls in the gap between them at around 1270 cm^{-1}. This reflects the coexistence of two different chemical bonds related to hydrogen in the material. The modes from 350 and 500 cm^{-1} are assigned as the CrH_7 librational motions and the remaining modes are related to the metal motions.

Among the zone-center optic phonon modes, there are a total of 105 IR-active modes ($35B_1 + 35B_2 + 35B_3$), which provide six H-related peaks in the calculated IR spectrum in Figure 4a. This is in excellent agreement with our experimental measurements, as is evident from a comparison of Figure 4a and b. We also confirmed experimentally that these peaks are indeed associated with the H vibrations through the peak shifts upon deuteration that are approximately scaled by a factor of $1/\sqrt{2}$, as indicated in Figure 4b and c. These results strongly support the formation of the first Group 6 hydride complex $[CrH_7]^{5-}$.

In summary, we have successfully synthesized the complex transition-metal hydride Mg_3CrH_8, containing the first Group 6 homoleptic hydride complex $[CrH_7]^{5-}$, based on first-principles prediction. We found strong hybridization between the 1s orbitals of seven H atoms and Cr spd orbitals in the CrH_7 unit, which is induced by the pentagonal-bipyramidal ligand field. In addition, the absence of occupation of any antibonding orbitals suggests covalent bonding between seven H atoms and Cr, which enables the formation of $[CrH_7]^{5-}$.

Given that the 4d and 5d transition metals have more extended d-orbitals that are expected to enhance the covalency with hydrogen, the above discussion would be true for the other Group 6 elements, molybdenum and tungsten. Furthermore, given that the early transition metals ranging from Group 3–5 favor ionic/metallic bonding with hydrogen, the true boundary for the formation of homoleptic transition-metal hydride complexes should lie between Groups 5 and 6. The current results will provide a crucial insight into the systematic understanding of the chemical bonding associated with hydrogen and pave the way for further discovery of hydrogen-rich materials that are of both technological and fundamental interest.

Keywords: chromium · hydride ligands · hydrides · structure elucidations · transition metals

How to cite: *Angew. Chem. Int. Ed.* **2015**, *54*, 5650–5653
Angew. Chem. **2015**, *127*, 5742–5745

[1] a) S. Orimo, Y. Nakamori, J. R. Eliseo, A. Züttel, C. M. Jensen, *Chem. Rev.* **2007**, *107*, 4111–4132; b) K. Miwa, S. Takagi, M. Matsuo, S. Orimo, *J. Phys. Chem. C* **2013**, *117*, 8014–8019; c) S. Takagi, T. D. Humphries, K. Miwa, S. Orimo, *Appl. Phys. Lett.* **2014**, *104*, 203901.

[2] a) N. W. Ashcroft, *Phys. Rev. Lett.* **2004**, *92*, 187002; b) M. I. Eremets, I. A. Trojan, S. A. Medvedev, S. J. Tse, Y. Yao, *Science* **2008**, *319*, 1506–1509; c) S. Iimura, S. Matuishi, H. Sato, T. Hanna, Y. Murabe, S.-W. Kim, J.-E. Kim, M. Takata, H. Hosono, *Nat. Commun.* **2012**, *3*, 943.

[3] a) M. Matsuo, S. Orimo, *Adv. Energy Mater.* **2011**, *1*, 161–172; b) T. Ikeshoji, Y. Ando, M. Otani, E. Tsuchida, S. Takagi, M. Matsuo, S. Orimo, *Appl. Phys. Lett.* **2013**, *103*, 133903; c) T. Ikeshoji, E. Tsuchida, S. Takagi, M. Matsuo, S. Orimo, *RSC Adv.* **2014**, *4*, 1366–1370.

[4] C. Tassel, Y. Goto, Y. Kuno, J. Hester, M. Green, Y. Kobayashi, H. Kageyama, *Angew. Chem. Int. Ed.* **2014**, *53*, 10377–10380; *Angew. Chem.* **2014**, *126*, 10545–10548.

[5] a) J. N. Huiberts, R. Griessen, J. H. Rector, R. J. Wijngaarden, J. P. Dekker, D. G. de Groot, N. J. Koeman, *Nature* **1996**, *380*, 231–234; b) K. Yvon, G. Renaudin, C. M. Wei, M. Y. Chou, *Phys. Rev. Lett.* **2005**, *94*, 066403.

[6] P. Vajeeston, P. Ravindran, A. Kjekshus, H. Fjellvåg, *Phys. Rev. B* **2004**, *69*, 020104(R); b) A. Aguayo, D. J. Singh, *Phys. Rev. B* **2004**, *69*, 155103; c) D. J. Singh, *Phys. Rev. B* **2005**, *71*, 216101; d) P. Vajeeston, P. Ravindran, A. Kjekshus, H. Fjellvåg, *Phys. Rev. B* **2005**, *71*, 216102.

[7] K. Hayashi, P. V. Sushko, Y. Hashimoto, A. L. Shluger, H. Hosono, *Nat. Commun.* **2014**, *5*, 3515.

[8] W. Bronger, *Angew. Chem. Int. Ed. Engl.* **1991**, *30*, 759–768; *Angew. Chem.* **1991**, *103*, 776–784.

[9] K. Yvon, *CHIMIA* **1998**, *52*, 613–619.

[10] a) E. Orgaz, *Phys. Rev. B* **2000**, *61*, 7989–7995; b) D. J. Singh, M. Gupta, R. Gupta, *Phys. Rev. B* **2007**, *75*, 035103; c) E. Orgaz, A. J. Aburto, *J. Phys. Chem. C* **2008**, *112*, 15586–15594; d) M. Matsuo, H. Saitoh, A. Machida, R. Sato, S. Takagi, K. Miwa, T. Watanuki, Y. Katayama, K. Aoki, S. Orimo, *RSC Adv.* **2013**, *3*, 1013–1016; e) S. Takagi, K. Miwa, T. Ikeshoji, R. Sato, M. Matsuo, G. Li, K. Aoki, S. Orimo, *J. Alloys Compd.* **2013**, *580*, S274–S277; f) S. Takagi, T. Ikeshoji, T. Sato, K. Aoki, S. Orimo, *J. Jpn. Inst. Met. Mater.* **2013**, *77*, 604–608; g) M. Gupta, D. J. Singh, R. Gupta, *Phys. Rev. B* **2005**, *71*, 092107.

[11] a) S. Takagi, T. Ikeshoji, M. Matsuo, T. Sato, H. Saitoh, K. Aoki, S. Orimo, *Appl. Phys. Lett.* **2013**, *103*, 113903; b) R. Hoffmann, B. F. Beier, E. L. Muetterties, A. R. Rossi, *Inorg. Chem.* **1977**, *16*, 511–522.

[12] a) A. L. Allred, *J. Inorg. Nucl. Chem.* **1961**, *17*, 215–221; b) A. L. Allred, E. G. Rochow, *J. Inorg. Nucl. Chem.* **1958**, *5*, 264–268.

[13] D. Moser, D. J. Bull, T. Sato, D. Noréus, D. Kyoi, T. Sakai, N. Kitamura, H. Yusa, T. Taniguchi, W. P. Kalisvaart, P. Notten, *J. Mater. Chem.* **2009**, *19*, 8150–8161.

[14] G. Markopoulos, P. Kroll, R. Hoffmann, *J. Am. Chem. Soc.* **2010**, *132*, 748–755.

[15] D. G. Westlake, *J. Less-Common Met.* **1983**, *91*, 275–292.

[16] CCDC 1044636 (Mg_3CrD_8) contains the supplementary crystallographic data for this paper. These data can be obtained free of charge from The Cambridge Crystallographic Data Centre via www.ccdc.cam.ac.uk/data_request/cif.

Received: January 27, 2015
Revised: February 13, 2015
Published online: March 13, 2015

